Int. J. Nano Dimens., 12 (1): 11-19, Winter 2021

ORIGINAL ARTICLE

Anticancer activity of Doxorubicin conjugated to polymer/carbon based-nanohybrid against MCF-7 breast and HT-29 colon cancer cells

Neda Hazhir [1], Fereshteh Chekin [1,], Jahan Bakhsh Raoof [2], Shahla Fathi [1]*

[1]*Department of Chemistry, Ayatollah Amoli Branch, Islamic Azad University, Amol, Iran*
[2]*Electroanalytical Chemistry Research Laboratory, Department of Analytical Chemistry, Faculty of Chemistry, University of Mazandaran, Babolsar, Iran*

Received 06 August 2020; revised 07 October 2020; accepted 08 October 2020; available online 10 October 2020

Abstract

The Cancer is one of the world's most devastating diseases. Doxorubicin (DOX) is an effective chemotherapeutic drug; however, its toxicity is a significant limitation in therapy. Due to the severe side effects of chemotherapy drugs, scientists have tried to load these drugs in nanocomposites. This paper describes a facile and low cost approach for preparation polymeric biodegradable nanohybrid based on doxorubicin loaded onto chitosan/porous reduced graphene oxide (DOX/CS-prGO). Raman spectroscopy, thermogravimetric analysis (TGA) and field emission scanning electron microscope images (FE-SEM) revealed DOX onto CS-prGO nanocomposite. In addition, the study reported here evaluated the cytotoxicity effects of DOX/CS-prGO on MCF-7 breast cancer and HT-29 colon cancer cell lines. Cytotoxicity tests showed significantly higher viability loss and toxicity of DOX/CS-prGO in comparison with CS-prGO against cancer cells especially for HT-29 colon cells (with cell viability of ~36%, ~29% and ~9% for 24, 48 and 72 h exposure, respectively). The viability loss of DOX/CS-prGO is comparable to that reported by free DOX. Thus, the development of nanohybrid based on polymer/carbon conjugated to DOX will remarkably enhance anticancer activity because of their unique physicochemical properties, high surface area and stronger inhibitory effect. These nanocomposites are an ideal candidate to deliver anticancer agents into cells.

Keywords: *Breast Cancer; Chitosan; Colon Cancer; Doxorubicin; Porous Reduced Graphene Oxide..*

How to cite this article

Hazhir N., Chekin F., Bakhsh Raoof J., Fathi Sh. Anticancer activity of Doxorubicin conjugated to polymer/carbon based-nanohybrid against MCF-7 breast and HT-29 colon cancer cells . Int. J. Nano Dimens., 2020; 12(1): 11-19.

INTRODUCTION

The cancer is the second cause of mortality after cardiovascular diseases [1, 2]. Cancer is defined as the abnormal and uncontrolled growth of the cells affected by complex genetic and epigenetic DNA changes [3, 4]. Chemotherapy is one of the most important ways to treatment of cancer. However, today, so many chemotherapy drugs are used to treat various cancers that their use is limited because of some drawbacks such as serious side effects, low water solubility, and short circulation time [5, 6]. One of the most serious issues is the nonselective nature of the chemotherapeutic drugs, which causes innumerable side effects [7]. These often kill healthy cells besides the cancerous ones and cause toxicity in the patient. It is therefore desirable to develop chemotherapeutics that can either passively or actively target only cancerous cells [8, 9]. In order to overcome the specific constraints of traditional chemotherapy methods and to achieve more efficient therapies, anticancer drugs should be loaded into hydrophilic, biocompatible and nontoxic nanocarriers, with more durability in blood circulation [10-12].

Doxorubicin (DOX), chemically recognized as an anthracycline molecule [13], is one of the most

* Corresponding Author Email: *fchekin@yahoo.com*

commonly used drugs in the treatment of various cancers, such as breast, ovarian and stomach [14]. Numerous clinical studies demonstrated that DOX can strikingly hinder the growth of tumor cells in various cellular growth cycles by inhibiting the synthesis of RNA and DNA [15]. However, effective inhibition can be achieved in a relatively smaller dose of DOX when compared with other anticancer drugs [16] but DOX usually induced side effects resulted from the lack of specific targeting for tumor cells and nonselective inhibition of DNA and RNA, which seriously limited the clinical applications [17, 18]. Therefore, an efficient delivery system for DOX should be developed to make DOX more specific and effective targeting, more easily to be encapsulated, an excellent intake capacity and biocompatibility [9]. In order to increase the anticancer efficacy by prolonging the circulation time in blood stream and reduce its toxicity, different carrier systems for DOX have been developed such as liposomes and polymeric nanomaterials [19, 20]. Furthermore, the nanocomposite forms allow DOX to remain in the circulation system for longer periods of time, which will allow delivering greater amount of the drug to cancerous cells or tumors [21-23]. Interactions between carbon nanomaterials and living organisms and their subsequent biological responses are one of the most active research fields in nanotoxicology [24, 25]. In the last few years, there has been a noticeable increase in medical applications of nanostructured carbon materials [26, 27].

The porous reduced carbon graphene oxide (prGO) possesses excellent mechanical strength, large surface area and high adsorption capability. It has driven to cancer nanotechnology to defeat cancer therapy obstacles, via integration into three-dimensional (3D) hydrogel network with biocompatible polymers as nanocomposites carrier, and controllable release of anticancer drugs [28]. Additionally, modification of prGO with various polymers such as natural polymers enhances its biodegradability, drug loading, and target delivery [29]. The functional group (COOH and OH) of prGO allows it to conjugate with various polymers and biomolecules (ligand, DNA, protein) [30]. This unique surface chemistry allows for π–π stacking interactions and electrostatic interaction to occur with drugs in drug delivery applications [31, 32].

The thermodynamic interaction force of the nanocomposite materials determines the composite materials suitability for physically modifying the polymer [33, 34]. The forces of interaction between the composite material molecules and polymer macromolecules should be greater than the forces of interaction between the composite material molecules themselves, otherwise the composite material molecules would become associated, leading to their migration from the polymer matrix [35, 36]. The Flory–Huggins theory plays an important role in assessing the mutual miscibility of the polymer and the composite material. The so-called Flory–Huggins parameter of mutual interaction is the criterion defining the miscibility of polymer with composite material. It allows for a quantification of the affinity of the composite material with the polymer [37-39]. Chitosan, a cationic, linear nitrogenous polysaccharide composed of glucosamine and N -acetyl-glucosamine linked by (1 → 4) β-glycoside bonds, is the second most abundant polymer in nature after cellulose. The main properties of chitosan such as biocompatibility, biodegradability and bioadhesiveness which facilitates the ionic interaction of positively charged amino groups of chitosan with negatively charged mucous layer are accountable for its usage as a promising matrix in pharmaceutical industry [40-42]. Drugs can be covalently conjugated to polymer nanocomposite carriers, which provide specific accumulation at the tumor site based on the enhanced permeability and retention effect [43]. Furthermore, cell recovery after the metabolization of polymer-based nanomaterials occurs easily in vivo, thanks to the very low contact time between healthy tissues and the biodegradation nanomaterials that are carried away from the degradation site by the blood flow [44]. The present work, therefore, is devoted to produce a new nanocomposite based on DOX/CS-prGO. The therapeutic effect of DOX/CS-prGO was also evaluated in vitro by measuring the viability of MCF-7 breast and HT-29 colon cancer cells (Fig. 1).

EXPERIMENTAL

Materials

Graphene oxide was purchased from Iranian Nano Materials Pioneers. Hydrogen peroxide (H_2O_2), sulfuric acid (H_2SO_4), hydrazine hydrate ($H_4N_2 \cdot H_2O$), sodium hydroxide (NaOH), potassium hexacyanoferrate (II) ($[K_4Fe(CN)_6]$), doxorubicin

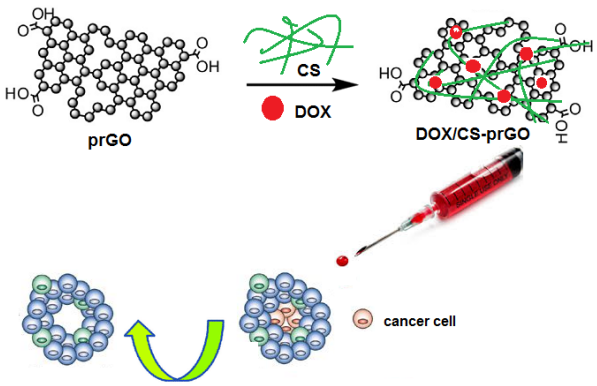

Fig. 1. Schematic illustration for the preparation of DOX/CS-prGO hybrid and its cytotoxicity effect on cancer cells.

hydrochloride ($C_{27}H_{29}NO_{11}$.HCl), phosphoric acid (H_3PO_4), sodium dihydrogen phosphate (NaH_2PO_4), disodium hydrogen phosphate (Na_2HPO_4), sodium phosphate (Na_3PO_4) and chitosan (medium molecular weight) were purchased from Sigma-Aldrich and used as received. The human breast (MCF-7) and colon (HT-29) cell lines were obtained from Pasteure Institute of Iran North Research Center.

Apparatus

Surface morphology and chemical composition of nanocomposite were examined by a scanning electron microscope of MIRATESCAN-XMU (Czech Republic) combined with EDX (energy-dispersive X-ray Spectroscopy) machine. UV-Vis spectra of samples were recorded by UV-Vis spectrophotometer (UV-1900, Shimadzu Co., Japan). Raman analysis was performed with a Takram P50C0R10 Raman spectrometer (Teksan, Iran) using a 532 nm laser and CCD array detector. Thermogravimetric analysis (TGA) analysis was carried out by STA 503 analyzer (Bahr, Germany) with 5 mg dried samples in a platinum pan under argon atmosphere from 25 to 800 °C. The heating rate was 10 °C min^{-1}. Electrochemical measurements were performed with a potentiostat/galvanostat (Metrohm Autolab, The Netherlands). A conventional three-electrode configuration consisting of Ag|AgCl|KCl3M as the reference electrode, a platinum wire as auxiliary electrode and DOX/CS-prGO modified GCE as working electrode was employed.

Preparation of DOX/CS-prGO nanohybrid

The prGO was prepared based on previous report [45, 46]. Briefly, 3 mg of graphene oxide (GO) in 5 mL of water was added and sonicated for 6 h at 25 °C and then hydrazine hydrate (0.5 mL, 25 M) was added to dispersed solution and heated in an oil bath for 20 h at 80 °C. The product (rGO) was filtrated, washed with water and ethanol and dried in the oven at 100 °C overnight. 3 mg of rGO was sonicated in 30 mL of H_2O_2 30 % for 30 min and refluxed for 12 h at 60 °C. The obtained solution was filtered and the recovered prGO powder was dialyzed to remove H_2O_2 and to separate from small sized graphene quantum dots. The product was kept for drying in an oven at 60 °C overnight.

1 mg of prGO was sonicated in 1 mL water for 1 h. Then, 0.5 mL of CS (0.5 mg/mL in 1% acetic acid) was added in prGO suspension solution and sonicated for 30 min at 25 °C. The product was filtered, washed with water and stored in fridge for using.

1 mg of CS-prGO nanocomposite in 2 mL phosphate buffer solution (PBS) 0.1 M with pH 7.00 was dispersed for 30 min at 25 ^{0}C. 0.5 mg of DOX to CS-prGO dispersed solution was added and the mixture was continuously stirred for 3 h at room temperature. The sample was then centrifuged (relative centrifugal force of 8000 g for 15 min) to separate solid phase (DOX/CS-prGO). The collected DOX/CS-prGO hybrid was washed with water, dried overnight at room temperature and stored in fridge for using.

Cytotoxicity assay

The human breast (MCF-7) and colon (HT-29) cell lines were cultured in RPMI 1640 medium containing 10% fetal bovine serum (FBS), penicillin (100 µg/ml), streptomycin (100 µg/ml) and glutamine (0.002 M) for 72 h at room temperature. The 3 mL of culture medium containing 8000 cells was placed to well plates and incubated at 37 °C in the atmosphere containing 5% CO_2 for 24 h. The

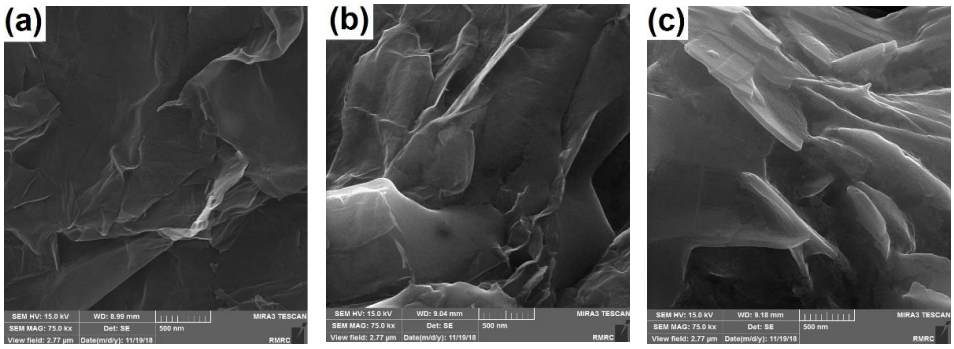

Fig. 2. FE-SEM images of prGO (a), CS-prGO (b) and DOX/CS-prGO (c).

different concentrations (0.08, 0.16, 0.31, 0.63, 1.25, 2.5 and 5 µg/ml) of free DOX, CS-prGO and DOX/CS-prGO samples were freshly prepared, then 200 µl of samples immediately treated to the cell lines for 24, 48 and 72 h. Cells not treated with samples served as controller.

A cytotoxicity evaluation of DOX, CS-prGO and DOX/CS-prGO samples was carried out on MCF-7 and HT-29, to study viability. The toxicity and cells viability were measured by exposure for different times with different concentrations of DOX, CS-prGO and DOX/CS-prGO. After 24, 48 and 72 h to exposure, the cells were washed, 200 µl of culture medium containing 0.5 mg MTT was added to well plates and incubated for 4 h at 37 °C. The colored crystals of formazan were formed due to the metabolism of tetrazolium. The well plates were replaced with 150 µl of DMSO. After 30 min extraction at room temperature, the absorbance of the formazan solution is read at 570 nm. The light absorbance of each well plate is a criterion for survival of cells, recorded by an ELISA reader. Viability was calculated using the following equation:

$$\%\text{Viability} = [(A_s - A_b) / (A_c - A_b)] \times 100 \quad (1)$$

Where A_b, A_c and A_s are the absorbance of blank, control and sample solutions, respectively.

Statistical analysis

Statistical analysis was performed by using the Student's t-test (SPSS version 7.5). Data with $P \leq 0.05$ and $P \leq 0.001$ were considered significant and very significant, respectively.

RESULTS AND DISCUSSIONS

Loading of DOX onto CS-prGO nanocomposite

The amount of DOX loaded onto CS-prGO nanocomposite in 0.1 M PBS (pH 7.00) at room temperature and shaking time of 3 h is determined on the basis of standard curve of DOX absorbance to its concentration at 480 nm. The loaded percent onto nanocomposite was calculated using the following equation:

$$\text{Loading}\% = [(C_{int} - C_s) / C_{int}] \times 100 \quad (2)$$

Where, C_{int} and C_s are the initial concentration and the supernatant concentration of DOX after loading, respectively. An efficient loading of DOX, 86% at pH 7.00 and time 3 h was observed onto CS-prGO. It is found that CS-prGO makes strong hydrogen binding with DOX due to the presence of –COOH, –OH and $–NH_2$ in CS-prGO.

FE-SEM and EDX study

The morphology of prGO, CS-prGO and DOX/CS-prGO is characterized with FE-SEM. As seen in Fig. 2, the prGO is a thin layer and smooth surface (Fig. 2a). In contrast, the surface of CS-rGO appears multilayered sheets and rougher surface structures (Fig. 2b). While stacking and protuberances are observed on the surface of DOX/CS-prGO nanohybrid (Fig. 2c) that this observation confirms the formation of DOX/CS-prGO nanohybrid. There are the π-π stacking interactions as well as the hydrophobic effect between DOX and CS-prGO in nanohybrid. Moreover, the –OH, $–NH_2$ and –COOH groups on CS-prGO nanocomposite form hydrogen binding interaction with –OH and $–NH_2$ of DOX.

TGA analysis

The samples were analyzed by TGA (Fig. 3a) to evaluate the thermal stability and successful forming of DOX/CS-prGO nanohybrid. The prGO showed much high stability with less weight loss up to 500 °C. The TGA curve of the prGO showed

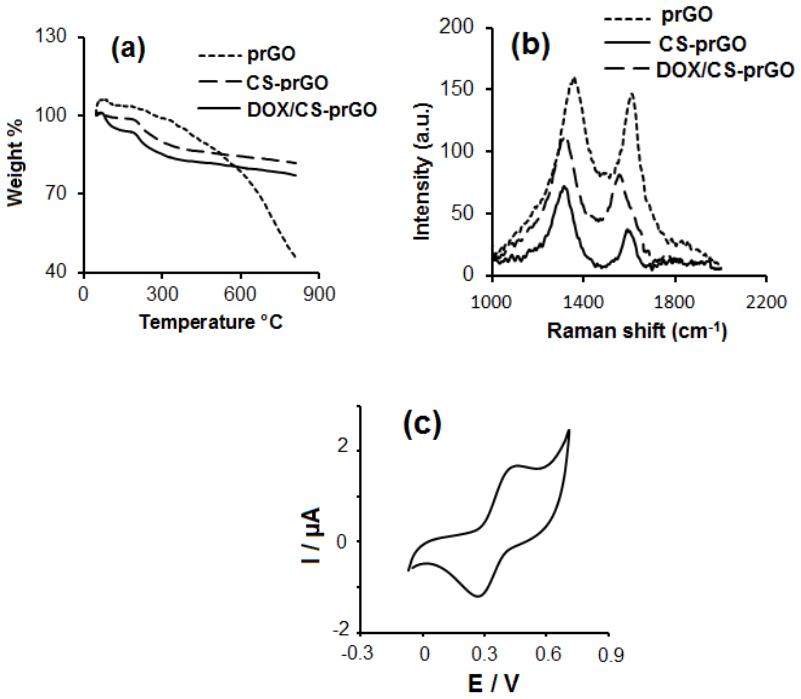

Fig. 3. TGA curves (a) and Raman spectra (b) of prGO, CS-prGO and DOX/CS-prGO; (c) cyclic voltammogram of DOX/CS-prGO modified GCE in 0.1 M PBS (pH 7.00) at scan rate of 50 mV s^{-1}.

~40% weight loss from 500 ˚C to 800 ˚C attributed to burning of carbon skeleton. The CS-prGO loses its weight in two steps. The first weight loss (~3 %) between 90 and 190 °C is loss of adsorbed water and functional groups (CO, CO_2, COOH and NH_2). The second step of weight loss (~13 %) from 190 to 500 °C is attributed to the loss of remaining functional groups of prGO and chains of CS. In the TGA curve of DOX/CS-prGO, one step mass loss ~7.5 % was observed at temperature between 90 and 190 °C attributed to adsorbed water and functional groups of DOX, CS and prGO. The ~13% weight loss in the temperature range 190–500 °C attributed to the loss of remaining functional groups.

Raman spectroscopy analysis

Raman spectroscopy was further employed to characterize of prGO, CS-prGO and DOX/CS-prGO (Fig. 3b). The Raman spectrum of prGO shows the D and G bands at 1361 and 1619 cm^{-1} with the intensity ratio of D and G bands (I_D/I_G) of 1.1. The D and G bands of CS-prGO are shifted to 1321 and 1602 cm^{-1}, and the I_D/I_G of prGO increased to 1.9 after the introduction of CS on prGO due to the amide linkage and removal of oxygen containing functional groups. Also, D and G bands of Dox/CS-prGO (with I_D/I_G of 1.5) shift to 1302 cm^{-1} and 1565 cm^{-1} due to decrease the number of free functional groups of CS-prGO after mixing with DOX indicating the deformation of ordered structure and the appearance of different groups.

Electrochemical test

The DOX/CS-prGO modified glassy carbon electrode (GCE) was prepared based on previous report [40]. Fig. 3c shows the cyclic voltammogram obtained at the DOX/CS-prGO modified GCE in 0.1 M PBS (pH 7.00). A pair of well-defined redox peaks was obtained in the cyclic voltammogram of the DOX/CS-prGO modified GCE. The anodic peak potential was observed at about 450 mV, and the cathodic peak potential at about 270 mV are ascribed to DOX onto CS-prGO nanocomposite oxidized according to Fig. 4 [47]:

The surface concentration of the electro-active DOX onto CS-prGO can be estimated using the equation [48]:

$$\Gamma = Q/nFA \quad (3)$$

Where Q is the charge consumed in coulombs, obtained from integrating the anodic (or cathodic)

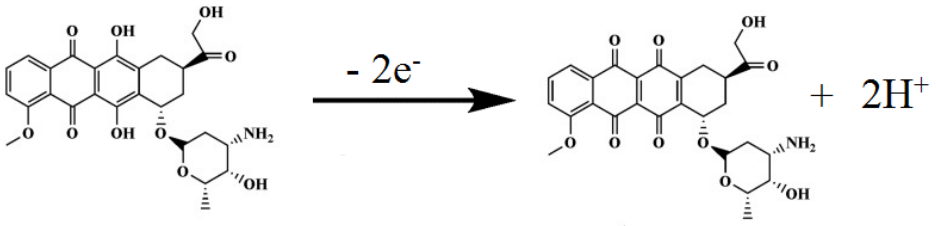

Fig. 4. The oxidation mechanism of DOX.

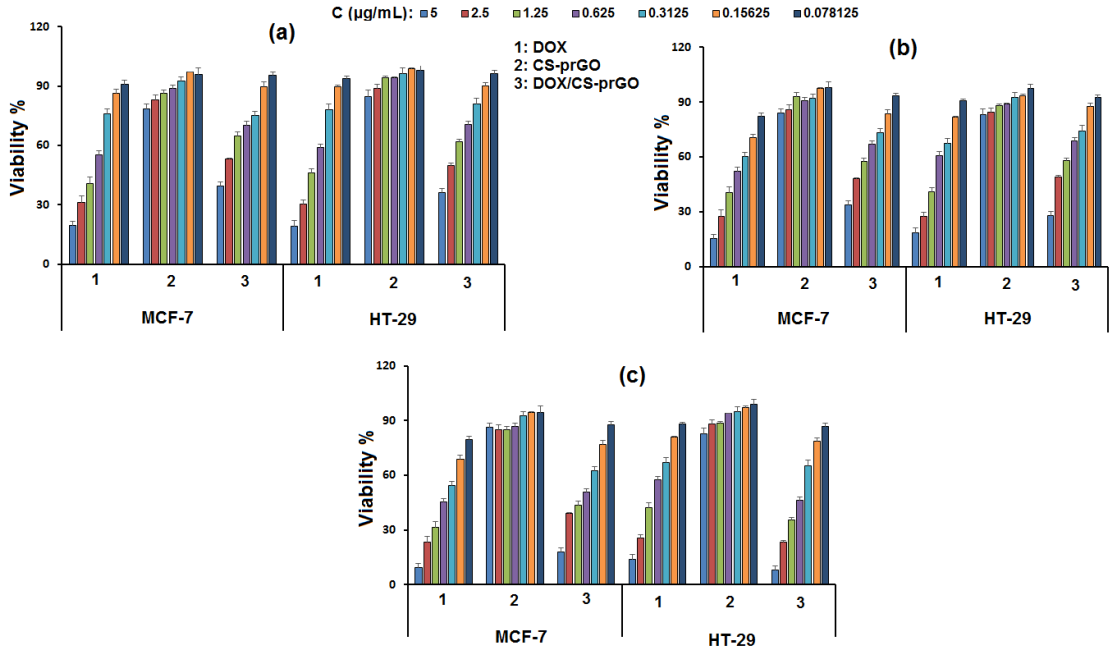

Fig. 5. The cell viability of MCF-7 and HT-29 cancer cells after treatment with free DOX, CS-prGO and DOX/CS-prGO for (a) 24, (b) 48 and (c) 72 h.

peak area in cyclic voltammogram under the background correction. The average value of (7.04 ± 0.72) × 10^{-11} mol/cm^2 was calculated.

In vitro cytotoxicity evaluation

The cell toxicity of free DOX, CS-prGO and DOX/CS-prGO with different concentrations on MCF-7 breast and HT-29 colon cell lines in three time intervals of 24, 48 and 72 h was evaluated by MTT assay to assess cell viability (Fig. 5a, 5b, 5c). According to the results of MTT assay, we didn't observe any significant toxicity for CS-prGO on the mentioned two cell lines, while free DOX and DOX/CS-prGO cause a significant decrease in the survival of the MCF-7 and HT-29 cell lines depending on dosage and time. The results revealed a good cytocompatibility of CS-prGO nanocomposite which showed low apparent toxicity against MCF-7 and HT-29 cells, even at higher concentrations (2.5 and 5 μg/mL), and the viability was above 80%. The treatment of free DOX for 24 h and 48 h to exposure showed most viability loss in both cell lines. The higher toxicity of free DOX was caused by more rapid passive diffusion in vitro, while the macromolecular conjugates (DOX/CS-prGO) internalized into cell mainly through less efficient endocytosis. After 72 h, an obvious decrease in cell viability with DOX/CS-prGO (5 μg/mL) was seen especially for HT-29 cells as much as about ~10%, whereas the toxicity effect of free DOX (~10%) on MCF-7 was smaller than DOX/CS-prGO (~20%). It is suggested that DOX/CS-prGO at long times has the high ability to penetrate from the cell member and deliver DOX which can lead to cell death.

The half-maximal inhibitory concentration (IC50) of free DOX and DOX/CS-prGO after 24, 48

Table 1. The IC50 (µg/mL) of free DOX and DOX/CS-prGO after 24, 48 and 72 h exposure against cell lines.

Time (h)	MCF-7 cells		HT-29 cells	
	DOX	DOX/CS-prGO	DOX	DOX/CS-prGO
24	0.64	6.63	0.70	4.91
48	0.44	3.75	0.58	3.17
72	0.33	1.33	0.50	0.89

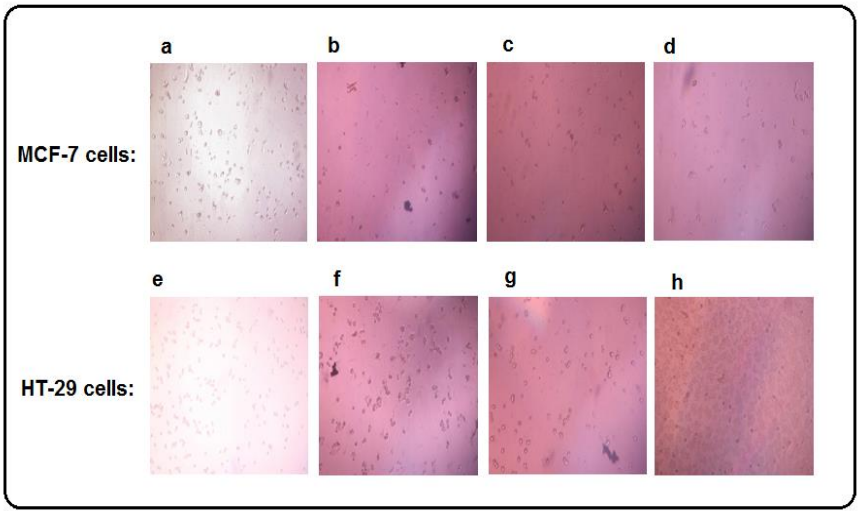

Fig. 6. The cell morphologies of MCF-7 and HT-29 cancer cells before (a and e) and after treatment with CS-prGO (b and f), free DOX (c and g) and DOX/CS-prGO (d and h) for 72 h.

and 72 h exposure against cell lines was illustrated in Table 1. It was found that IC50 value of CS-prGO was very high against both of cell lines and suggested that CS-prGO because of rich functional groups on the surface did not diminish the viability of cell lines. For DOX/CS-prGO after 24, 48 and 72 h exposure, the IC50 values for HT-29 cell lines were found to be lower than that observed for MCF-7 cells. This result reveals that DOX/CS-prGO showed enhanced anticancer capability against HT-29 cell.

In addition, the cell morphologies of MCF-7 and HT-29 cell lines after treatment with free DOX, CS-prGO and DOX/CS-prGO for 72 h were observed by a light microscope (Fig. 6a-6h) and the results revealed that the number of treated cells with free DOX and DOX/CS-prGO were obviously reduced as compared to the control sample. Thus, the viability loss and toxicity of DOX/CS-prGO is significantly high against cells and acts as anticancer agent.

CONCLUSION

In the present work, after the loading the DOX on CS-prGO nanocomposite, we studied the effects of this nanocomposite on MCF-7 breast and HT-29 colon cancer cell lines. MTT assay was used to evaluate the anticancer effects of free DOX, CS-prGO and DOX/CS-prGO against cancer cell lines. The results showed that the prGO/CS nanocomposite had low toxic effect on the cell lines. DOX/CS-prGO due to the DOX onto CS-prGO composite sheets lead to the significant viability loss and toxicity on cancer cells specially against HT-29 cell. The viability loss of DOX/CS-prGO is comparable to that reported by free DOX. The results suggest that the present polymer/carbon nanohybrid will pave the way for a new approach to prevent and treat cancer.

ACKNOWLEDGMENT

The authors are sincerely thankful for the

research facilities provided by the Ayatollah Amoli Branch of the Islamic Azad University.

CONFLICT OF INTEREST

The authors declare that they have no competing interests.

REFERENCES

[1] Shahidi F., Hashemianzadeh S. M., (2018), Computational study of carbon, silicon and boron nitride nanotubes as drug delivery vehicles for anti-cancer drug temozolomide. *Am. J. Nanotechnol. Nanomed*. 1: 048–054.

[2] Iannazzo D., Pistone A., Celesti C., Triolo C., Patané S., Giofré S. V., Romeo R., Ziccarelli I., Mancuso R., Gabriele B., Visalli G., Facciolà A., Pietro A. D., (2019), A smart nanovector for cancer targeted drug delivery based on graphene quantum dots. *Nanomater*. 9: 282–298.

[3] Lichota A., Gwozdzinski K., (2018), Anticancer activity of natural compounds from plant and marine environment. *Int. J. Mol. Sci*. 19: 3533–3569.

[4] Amiri Z., Forouzandeh Moghadam M., Sadeghizadeh M., (2018), Anticancer effects of doxorubicin-loaded micelle on MCF-7 and MDAMB-231, breast cancer cell lines. *J. Res. Med. Dent. Sci*. 6: 298–304.

[5] Morad S. A., Levin J. C., Tan S. F., Fox T. E., Feith D. J., Cabot M. C., (2013), Novel off-target effect of tamoxifen - Inhibition of acid ceramidase activity in cancer cells. *Biochim. Biophys. Acta* 12: 1657–1664.

[6] Bourzac K., (2012), Nanotechnology carrying drugs. *Nature*. 491: 58–60.

[7] Parveen S., Sahoo S. K., (2010), Evaluation of cytotoxicity and mechanism of apoptosis of doxorubicin using folate-decorated chitosan nanoparticles for targeted delivery to retinoblastoma. *Cancer Nano.* 1: 47–62.

[8] Pilco-Ferreto N., Calaf G. M., (2016), Influence of doxorubicin on apoptosis and oxidative stress in breast cancer cell lines. *Int. J. Oncology*. 49: 753–762.

[9] Abdullahi Kamba S., Ismail M., Hussein-Al-Ali S. H., Tengku Ibrahim T. A., Bakar Zakaria Z. A., (2013), Invitro delivery and controlled release of Doxorubicin for targeting osteosarcoma bone cancer. *Molecules*. 18: 10580–10598.

[10] Hu C. M. J., Zhang L., (2012), Nanoparticle-based combination therapy toward overcoming drug resistance in cancer. *Biochem. Pharmacol*. 83: 1104–1111.

[11] Saadatmand M. M., Yazdanshenas M. E, Khajavi R., Mighani F., Toliyat T., (2019), Patterning the surface roughness of a nano fibrous scaffold for transdermal drug release. *Int. J. Nano Dimens*. 10: 78–88.

[12] Adebayo-Tayo B. C., Amaka Inem S., Ademola Olaniyi O., (2019), Rapid synthesis and characterization of Gold and Silver nanoparticles using exopolysaccharides and metabolites of Wesiella confusa as an antibacterial agent against *Esherichia coli. Int. J. Nano Dimens*. 10: 37–47.

[13] Gumulec J., Fojtu M., Raudenska M., Sztalmachova M., Skotakova A., Vlachova J., Skalickova S., Nejdl L., Kopel P., Knopfova L., Adam V., Kizek R., Stiborova M., Babula P., Masarik M., (2014), Modulation of induced cytotoxicity of Doxorubicin by using Apoferritin and Liposomal cages. *Int. J. Molec. Sci*. 15: 22960–22977.

[14] Matvienko T., Sokolova V., Prylutska S., Harahuts Y., Kutsevol N., Kostjukov V., Evstigneev M., Prylutskyy Y., Epple M., Ritter U., (2019), In vitro study of the anticancer activity of various doxorubicin containing dispersions. *BioImpacts*. 9: 57–63.

[15] Zhang G., Zhang Z., Yang, J., (2017), DNA tetrahedron delivery enhances Doxorubicin-induced apoptosis of HT-29 colon cancer cells. *Nanoscale Res. Lett*. 12: 495–502.

[16] Katuwavila N. P., Chandani Perera A. D. L., Samarakoon S. R., Soysa P., Karunaratne V., Amaratunga G. A. J., Nedra Karunaratne D., (2016), Chitosan-Alginate nanoparticle system efficiently delivers Doxorubicin to MCF-7 cells. *J. Nanomater*. 2016: 1–12.

[17] Chen Y., Wan Y., Wang Y., Zhang H., Jiao Z., (2011), Anticancer efficacy enhancement and attenuation of side effects of doxorubicin with titanium dioxide nanoparticles. *Int. J. Nanomed*. 6: 2321–2326.

[18] Filyak Y., Filyak O. S. S., Stoika R., (2008), Doxorubicin inhibits TGF-beta signaling in human lung carcinoma A549 cells. *Eur. J. Pharmacol*. 590: 67–73.

[19] Cabeza L., Ortiz R., Arias J. L., Prados J., Ruiz Martinez M. A., Entrena J. M., Luque R., Melguizo C., (2015), Enhanced antitumor activity of doxorubicin in breast cancer through the use of poly (butylcyanoacrylate) nanoparticles. *Int. J. Nanomed*. 10: 1291–1306.

[20] He S., Zhou Z., Li L., Yang Q., Yang Y., Guan S., Zhang J., Zhu X., Jin Y., Huang Y., (2016), Comparison of active and passive targeting of Doxorubicin for somatostatin receptor 2 positive tumor models by octreotide-modified HPMA copolymer-doxorubicin conjugates. *Drug Deliv*. 23: 285–296.

[21] Sabeti B., Noordin M. I., Mohd S., Hashim R., Dahlan A., Akbari Javar H., (2014), Development and characterization of liposomal Doxorubicin hydrochloride with palm oil. *Bio. Med. Res. Int*. 2014: 1–6.

[22] Redig A. J., Mc Allister S. S., (2013), Breast cancer as a systemic disease: A view of metastasis. *J. Int. Med*. 274: 113–126.

[23] Toldo S., Goehe R. W., Lotrionte M., Mezzaroma E., Sumner E. T., Biondi-Zoccai G. G. L., Seropian I. M., Van Tassell B. W., Loperfido F., Palazzoni G., Voelkel N. F., Abbate A., Gewirtz D. A., (2013), Comparative cardiac toxicity of anthracyclines in vitro and in vivo in the mouse. *PLOS One*. 8: 1–8.

[24] Kavinkumar T., Varunkumar K., Ravikumar V., Manivannan S., (2017), Anticancer activity of graphene oxide-reduced graphene oxide-silver composites. *J. Colloid Interf. Sci*. 505: 1125–1133.

[25] Zhang X., Hu W., Li J., Tao L., Wei Y., (2012), A comparative study of cellular uptake and cytotoxicity of multi-walled carbon nanotubes, graphene oxide, and nanodiamond. *Toxicol. Res*. 1: 62–68.

[26] Gu X., Cao R., Li F., Li Y., Jia H., Yu H., (2018), Graphene oxide as a nanocarrier for controlled loading and targeted delivery of Typhonium giganteum drugs. *J. Chem*. 2018: 1–7.

[27] Mirzaei M., (2013), Effects of carbon nanotubes on properties of the fluorouracil anticancer drug: DFT studies of a CNT-fluorouracil compound. *Int. J. Nano Dimens*. 3: 175–179.

[28] Karimzadeh Z., Javanbakht S., Namazi H., (2019), Carboxymethylcellulose/MOF-5/graphene oxide bio-nanocomposite as antibacterial drug nanocarrier agent. *BioImpacts.* 9: 5–13.

[29] Casais-Molina M. L., Cab C., Canto G., Medina J., Tapia A.,

(2018), Carbon nanomaterials for breast cancer treatment. *J. Nanomater*. 2018: 1–9.

[30] Usman M. S., Hussein M. Z., Kura A. U., Fakurazi S., Masarudin M. J., Ahmad Saad F. F., (2018), Graphene oxide as a nanocarrier for a theranostics delivery system of protocatechuic acid and Gadolinium/Gold nanoparticles. *Molecules.* 23: 500–516.

[31] Tadyszak K., Wychowaniec J. K., Litowczenko J., (2018), Biomedical applications of graphene-based structures. *Nanomater*. 8: 944–964.

[32] Zhang Q., Wu Z., Li N., Pu Y., Wang B., Zhang T., Tao J., (2017), Advanced review of graphene-based nanomaterials in drug delivery systems: Synthesis, modification, toxicity and application. *Mater. Sci. Eng. C*. 77: 1363–1375.

[33] Rana D., Bag K., Bhattacharyya S. N., Mandal B. M., (2000), Miscibility of poly(styrene-co-butyl acrylate) with poly(ethyl methacrylate): Existence of both UCST and LCST. *J. Polym. Sci. Polym. Phys. Ed.* 38: 369–375.

[34] Rana D., Kim H. L., Kwag H., Choe S., (2000), Hybrid blends of similar ethylene 1-octene copolymers. *Polym.* 41: 7067–7082.

[35] Rana D., Cho K., Woo T., Lee B. H., Choe S., (1999), Blends of ethylene 1-octene copolymer synthesized by Ziegler-Natta and metallocene catalysts. I. Thermal and mechanical properties. *J. Appl. Polym. Sci.* 74: 1169–1177.

[36] Rana D., Cho K., Lee B. H. Choe S., (1998), Is metallocene polyethylene blend with HDPE more compatible than with PP?. *Annual Tech. Conf.- ANTEC.* 2: 2462–2465.

[37] Rana D., Mandal B. M., Bhattacharyya S. N., (1996), Analogue calorimetric studies of blends of poly(vinyl ester) s and polyacrylates. *Macromol.* 29: 1579–1583.

[38] Rana D., Mandal B. M., Bhattacharyya S. N., (1996), Analogue calorimetry of polymer blends: Poly(styrene-co-acrylonitrile) and poly(phenyl acrylate) or poly(vinyl benzoate). *Polym.* 37: 2439–2443.

[39] Rana D., Mandal B. M., Bhattacharyya S. N., (1993), Miscibility and phase diagrams of poly(phenyl acrylate) and poly(styrene-co-acrylonitrile) blends. *Polym.* 34: 1454–1459.

[40] Yuan H., Meng L. Y., Park S. J., (2016), Synthesis and applications of graphene/chitosan nanocomposites. *Carbon Lett*. 17: 11–17.

[41] Tiwari S., Marathe S., Chandola M., Thakur N., Rathore R., Garg S., (2016), Synthesis and characterization of nanocomposites for drug delivery applications. *J. Polym. Textile Eng*. 3: 1–7.

[42] Li J., Cai C., Li J., Sun T., Wang L., Wu H., Yu G., (2018), Chitosan-based nanomaterials for drug delivery. *Molecules.* 23: 2661–2687.

[43] Pardo J., Peng Zh., Leblanc R. M., (2018), Cancer targeting and drug delivery using carbon-based quantum dots and nanotubes. *Molecules*. 23: 378–398.

[44] Vauthier C., Dubernet C., Chauvierre C., Brigger I., Couvreur P., (2003), Drug delivery to resistant tumors: The potential of poly (alkyl cyanoacrylate) nanoparticles. *J. Control. Release.* 93: 151–160.

[45] Zareyy B., Chekin F., Fathi Sh., (2019), NiO/porous reduced graphene oxide as active hybrid electrocatalyst for oxygen evolution reaction. *Russ. J. Electrochem*. 55: 333–338.

[46] Chekin F., Singh S. K., Vasilescu A., Dhavale V. M., Kurungot S., Boukherroub R., Szunerits S., (2016), Reduced graphene oxide modified electrodes for sensitive sensing of Gliadin in food samples. *ACS Sens*. 1: 1462–1470.

[47] Chekin F., Myshin V., Ye R., Melinte S., Singh S. K., Kurungot S., Boukherroub R., Szunerits S., (2019), Graphene-modified electrodes for sensing doxorubicin hydrochloride in human plasma. *Anal. Bioanal. Chem*. 411: 1509–1516.

[48] Chekin F., Vahdat S. M., Asadi M. J., (2016), Green synthesis and characterization of cobalt oxide nanoparticles and its electrocatalytic behavior. *Russ. J. Appl. Chemi*. 89: 816–822.